

Fully dense anisotropic nanocomposite $\text{Sm}(\text{Co}, \text{Fe}, \text{Zr}, \text{Cu}, \text{B})_z$ ($z=7.5-12$) magnets

M. Q. Huang,^{a)} Z. Turgut, and B. Wheeler
UES Inc., 4401 Dayton-Xenia Road, Dayton, Ohio 45432

D. Lee and S. Liu
University of Dayton Magnetic Laboratory, 300 College Park, Dayton, Ohio 45469

B. M. Ma
Magnequench Inc., 61 Science Park Road, 01-17 Galen, Singapore 117525

Y. G. Peng, S. Y. Chu, and D. E. Laughlin
Department of Materials Science and Engineering (MSE), Carnegie Mellon University, Pittsburgh, Pennsylvania 15213

J. C. Horwath and R. T. Fingers
Air Force Research Laboratory (AFRL), Wright-Patterson Air Force Base, Ohio 45433

(Presented on 9 November 2004; published online 11 May 2005)

Fully dense anisotropic nanocomposite $\text{Sm}(\text{Co}_{0.58}\text{Fe}_{0.31}\text{Zr}_{0.05}\text{Cu}_{0.04}\text{B}_{0.02})_z$ ($z=7.5-12$) magnets have been synthesized via rapid hot pressing and hot deformation processes. The highest $(\text{BH})_{\text{max}} \sim 10.6$ MGOe was observed for a magnet with $z=10$. X-ray diffraction and $M-H$ measurements indicated that the easy magnetization direction of magnets prefers to be in the hot pressing direction. Transmission electron microscopy investigation confirmed that plastic deformation is an important route for forming magnetic anisotropy in the Sm-Co-type nanocomposite magnets. Some stripe and/or platelike patterns have been observed inside the nanograins (50–200 nm), which may present as twins, and stacking faults. The (0001) twins have been observed in the 2:17R phase. © 2005 American Institute of Physics. [DOI: 10.1063/1.1851432]

INTRODUCTION

Nanocomposite $\text{Sm}_2\text{Co}_{17}/\text{Co}$ -based magnets have gained much attention in recent years because of their potential applications at elevated temperature. Many efforts have been devoted to produce nanocomposite powders, thin films, and rapidly quenched ribbons.¹⁻⁴ However, fabrication of anisotropic bulk nanocomposite magnets still remains a great challenge. Recently, fully dense nanocomposite magnets of $(\text{Sm}, \text{Gd})_2(\text{Co}, \text{Fe})_{17}/(\text{Co}, \text{Fe})$ have been successfully produced by rapid hot pressing of amorphous powder.⁵ However, they are magnetically isotropic even after hot deformation with a 60% height reduction. Thus, we believe that it is important to develop a suitable crystallographic texture during hot deformation, forming anisotropic nanocomposite Sm-Co-type magnets. In the present work, our objective is to synthesize fully dense anisotropic nanocomposite Sm-Co-based magnets via rapid hot pressing and hot deforming the melt-spun materials with compositions of $\text{Sm}(\text{Co}_{0.58}\text{Fe}_{0.31}\text{Zr}_{0.05}\text{Cu}_{0.04}\text{B}_{0.02})_z$ ($z=7.5-12$). These melt-spun materials have been reported in our previous work, exhibiting attractive hard magnetic properties and a suitable microstructure.^{6,7} In this paper, magnetic properties, phases present, crystallographic texture formation, and microstructure of fully dense nanocomposite magnets $\text{Sm}(\text{Co}_{0.58}\text{Fe}_{0.31}\text{Zr}_{0.05}\text{Cu}_{0.04}\text{B}_{0.02})_z$ will be reported.

EXPERIMENTAL DETAILS

As cast melt-spun ribbon powders with a nominal composition of $\text{Sm}(\text{Co}_{0.58}\text{Fe}_{0.31}\text{Zr}_{0.05}\text{Cu}_{0.04}\text{B}_{0.02})_z$ ($z=7.5-12$) were hot pressed (HP) at 750 °C for 30 s under 25 kpsi, followed by a hot deformation (HD) process at 900 °C for 3–5 min under 5–8 kpsi to form fully dense anisotropic nanocomposite magnets. The magnet specimens were around 12 mm in diameter. Curie temperatures (T_c) and hard magnetic properties [$4\pi M_r$, H_c , and $(\text{BH})_{\text{max}}$] at room tempera-

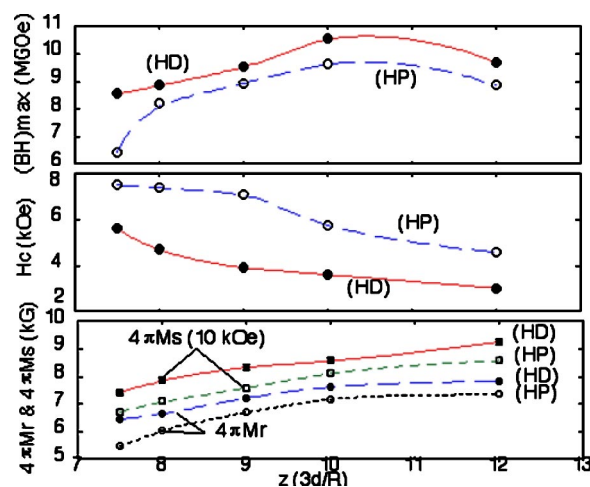


FIG. 1. Hard magnetic properties [H_c , $4\pi M_r$, $4\pi M_s$, and $(\text{BH})_{\text{max}}$] of $\text{Sm}(\text{Co}_{0.58}\text{Fe}_{0.31}\text{Zr}_{0.05}\text{Cu}_{0.04}\text{B}_{0.02})_z$ ($z=7.5-12$) magnets. (HP-hot pressed, HD-hot deformed).

^{a)}Electronic mail: meiqing.huang@wpaaf.af.mil

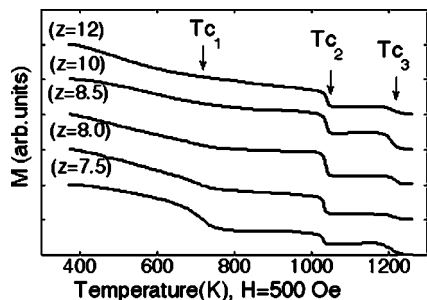


FIG. 2. M - T of hot-deformed $\text{Sm}(\text{Co}_{0.58}\text{Fe}_{0.31}\text{Zr}_{0.05}\text{Cu}_{0.04}\text{B}_{0.02})_z$ ($z = 7.5$ – 12) magnets.

ture were measured by a vibrating-sample magnetometer (VSM) and a hysteresisgraph. X-ray diffraction (XRD) with Cu radiation and transmission electron microscopy (TEM) were used to determine the crystal structure, phases present, crystallographic texture formation, and microstructure.

RESULTS AND DISCUSSIONS

Fully dense nanocomposite $\text{Sm}(\text{Co}_{0.58}\text{Fe}_{0.31}\text{Zr}_{0.05}\text{Cu}_{0.04}\text{B}_{0.02})_z$ ($z = 7.5$ – 12) magnets with a density of 8.23 – 8.27 g/cm^3 were obtained via HP and HD processing. The magnetic properties as functions of z are summarized in Fig. 1. Isotropic magnets with magnetic properties of $H_c \sim 4.6$ – 7.5 kOe , $B_r \sim 5.5$ – 7.4 kG , and $(\text{BH})_{\text{max}} \sim 6.4$ – 8.9 MGOe were formed after hot pressing at 750°C . Subsequently, anisotropic magnets, with magnetic properties of $H_c \sim 3$ – 5.7 kOe , $B_r \sim 6.4$ – 7.9 kG , and $(\text{BH})_{\text{max}} \sim 8.5$ – 10.6 MGOe with a 50%–60% height reduction were obtained after hot deformation at 900°C . The highest $(\text{BH})_{\text{max}} \sim 10.6 \text{ MGOe}$ was observed for a magnet with a composition of $z = 10$. XRD analysis on random powders indicated that all magnets comprised a mixture of three phases, 2:17R ($\text{Th}_2\text{Zn}_{17}$ -type), 1:7H (TbCu_7 -type) or 1:5H (CaCu_5 -type), and a small amount of $(\text{Co,Zr})_{23}\text{B}_6$. Figure 2 shows their Curie temperatures, T_{c1} , T_{c2} , and T_{c3} , corresponding to the 1:7 or 1:5, 2:17, and 6:23 phases, respectively. We have observed that the main phase changes from 2:17R in the magnet with $z = 12$ to 1:7H or 1:5H in the magnet with $z = 7.5$, resulting in higher B_r with lower H_c in the $z = 12$ magnet. The reverse is observed in the $z = 7.5$ magnet. The above information on the variation of phases present and magnetic properties with z ($3d/R$) are similar to that observed in the related ribbons,^{6,7} except that the structure-type of the 2:17 phase converts from $\text{Th}_2\text{Ni}_{17}$ in ribbons to $\text{Th}_2\text{Zn}_{17}$ after hot pressing.

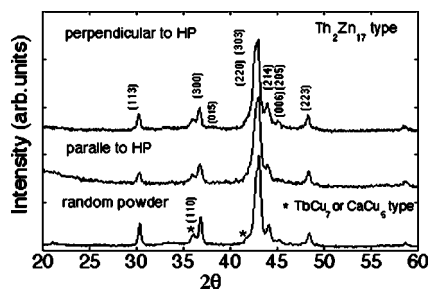


FIG. 3. XRD of hot-pressed isotropic magnet ($z = 10$).

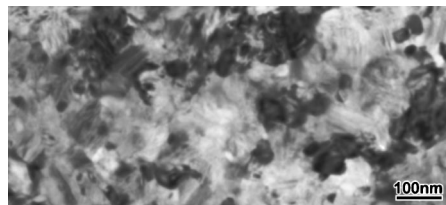


FIG. 4. TEM image of hot-pressed isotropic magnet ($z = 10$).

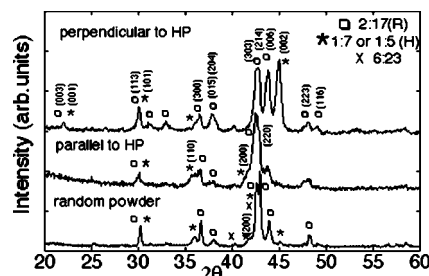


FIG. 5. XRD of hot-deformed anisotropic magnet ($z = 10$).

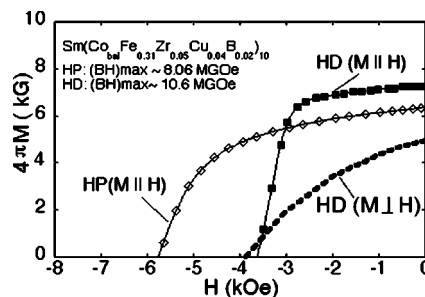


FIG. 6. Demagnetization curves of hot-pressed isotropic and hot-deformed anisotropic magnets ($z = 10$).

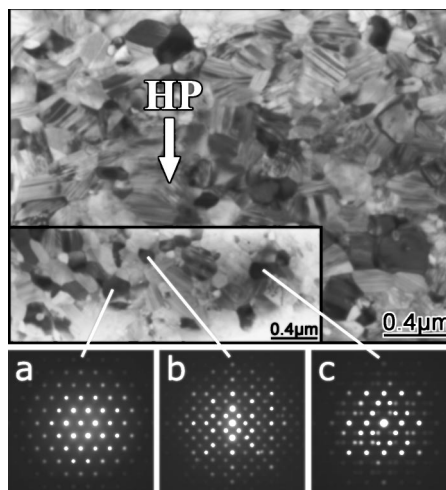


FIG. 7. TEM image and SAED of hot-deformed anisotropic magnet ($z = 10$). (a) $[0001]$ 1:7H (TbCu_7) or 1:5H (CaCu_5), (b) $[10\text{-}11]$ 2:17R ($\text{Th}_2\text{Zn}_{17}$), and (c) $[0001]$ twins of 2:17R.

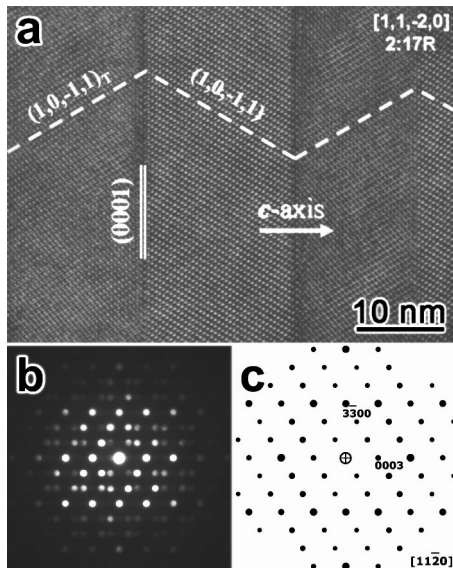


FIG. 8. (a) HRTEM image of (0001) twins of 2:17 phase of the hot-deformed anisotropic magnet ($Z=10$), (b) nanobeam electron-diffraction pattern of (0001) twins of 2:17R phase, and (c) index of one of the twin domains.

Our analysis is focused on the $z=10$ magnet, including anisotropy of magnetic properties, crystallographic texture formation, and microstructure. After hot pressing, as seen in Figs. 3 and 4, the magnets consist of nanograins of 50–100 nm, exhibiting an isotropic magnetic character with no evidence of crystallographic texture. During hot deformation processing, we found that a crystallographic texture developed with an increasing degree of deformation. The height reduction varies from 0 (HP) up to 56%–67% (HD). In the HD state, both XRD and M - H measurements indicate that the easy magnetization direction of magnets prefers to be in the hot pressing direction. As can be seen in Fig. 5, the XRD pattern on a surface perpendicular to the hot pressing direction shows that the diffraction peaks (003), (105), and (006), characteristic of the 2:17R phase, and (002), characteristic of the 1:7H or 1:5H phase, were strengthened significantly. This means that the c axis in both the 2:17 and 1:7

or 1:5 unit cells has been partially aligned along the hot pressing direction, i.e., perpendicular to the plastic deformation direction. As a result, as shown in Fig. 6, the $M_r(\text{hard})/M_r(\text{easy})$ ratio derived from the demagnetization curves along the two different magnetization directions is about 0.6. Further improvement in reducing misalignment will be needed.

TEM investigation also confirmed that a plastic deformation may have occurred by twinning and/or slipping of crystallographic planes during hot deformation and is an important route in forming a crystallographic texture (or anisotropy) in the Sm–Co-type nanocomposite magnets. As seen in Fig. 7, some stripe and/or platelike patterns partially along the plastic deformation direction have been observed inside the nanograins (50–200 nm), which may be present as twins, stacking faults, and/or Z phase. As can be seen in Fig. 8, an image of (0001) twins of the 2:17R phase and its nanobeam electron diffraction pattern have been successfully obtained via high-resolution transmission electron microscopy (HRTEM) investigation. Selected area electron-diffraction (SAED) patterns indicate that the 2:17R and 1:7 or 1:5H phases are detected in the magnet. Moreover, the results obtained via TEM mapping are consistent with that obtained by XRD and SAED. They are in good agreement with the magnet with $z=10$. Only one platelike Zr-rich phase was unaccounted for by the cross comparison. This Zr-rich phase may play an important role in developing H_c as does the Z phase in sintered Sm–Co magnets.⁸

¹S. K. Chen, J. L. Tsai, and T. S. Chin, *J. Appl. Phys.* **79**, 5964 (1996).

²C. Chen, S. Kodat, M. H. Walmer, S. F. Cheng, M. A. Willard, and V. G. Harris, *J. Appl. Phys.* **93**, 7966 (2003).

³B. Z. Cui, M. Q. Huang, and S. Lui, *IEEE Trans. Magn.* **39**, 2866 (2003).

⁴S. S. Makridis, G. Litsardakis, K. G. Efthimiadis, S. Hofinger, J. Fidler, and D. Niarchos, *J. Magn. Magn. Mater.* **272–276**, e1921 (2004).

⁵C. Chen, D. Lee, S. Lui, M. H. Walmer, Y. Zhang, and G. Hadjipanayis, *IEEE Trans. Magn.* **40**, 2937 (2004).

⁶M. Q. Huang *et al.*, *IEEE Trans. Magn.* **40**, 2934 (2004).

⁷R. Gopalan, D. H. Ping, K. Hono, M. Q. Huang, B. R. Smith, Z. Chen, and B. M. Ma, *J. Appl. Phys.* **95**, 4962 (2004).

⁸X. Y. Xiong, T. Ohkubo, T. Koyama, K. Phashi, Y. Tawara, and K. Hono, *Acta Mater.* **52**, 737 (2004).